

Investigation of the Existence of Thermal Insulations in Wall Systems of Building Envelopes Using UWB Technique

Saleh A. Alshehri*

Abstract—Hybrid pattern recognition is used to predict the types of insulation materials used inside wall systems of building envelopes. The hybrid pattern recognition features vector is built using the characteristics of UWB signals. UWB signals can penetrate objects, resulting in scattered signals based on the object's dielectric properties. The object's dielectric properties and structure have a signature within the scattered signals. This paper demonstrates that proper hybrid pattern recognition can be used to experimentally detect the existence and the type of insulation material inside wall systems with a high success rate.

1. INTRODUCTION

Commercial and residential buildings usually consume most of the energy. In the USA, it can reach up to 48% of the total energy use [1]. Energy consumption of the building sector is high, and although the situation differs from country to country, buildings are responsible for about 30–40% of the total energy demand [2]. In Europe, however, buildings are responsible for 40–50% of energy use, and the largest share of energy in buildings is used for heating [3]. The design of building enclosures with the intent of achieving energy savings can necessarily help reduce building operating loads and, thus, the demand for energy over time [4–13]. Thermal insulations are major contributors and obviously are a practical and logical first step towards achieving energy efficiency especially in envelope-load dominated buildings located in sites with harsh climatic conditions [4–13]. This can evidently be achieved by increasing the thermal resistance (R-value) of the building envelope.

One of the requirements of Saudi's electricity power service provider is to check whether the roofing and wall systems in building envelopes have adequate thermal insulation materials before allowing them to use electrical services. The challenge is that, after constructing the building, it is not appropriate to break parts of the roofing and wall systems to investigate whether the building envelope has an adequate level of thermal insulation that complies with the requirements of Saudi's building code. The overall thermal resistance (R-value) of a wall system can be measured using the guarded hot box (GHB) in accordance to the standard test method ASTM C-1363 [14]. It is obvious that this test method cannot be used to measure the R-value of a wall system in constructed buildings. Madding introduced a technique that can be used to measure the R-value of a wall in constructed buildings using infrared thermography [15]. This technique, however, requires not only subjecting the wall systems to temperature differences (ΔT) but also the measured R-value was found to be significantly dependant on both its value and ΔT . As such, Madding technique cannot be used to measure the R-value of a newly-constructed building (i.e., without having the electrical service that is needed to create ΔT across the test sample). In this paper, a technique is introduced to investigate the existence and type of thermal insulation in a wall system.

Received 28 August 2016, Accepted 22 November 2016, Scheduled 29 November 2016

* Corresponding author: Saleh A. Alshehri (shehri@ucj.edu.sa).

The author is with the Department of Computer Science & Engineering, Jubail University College, Jubil Industrial City, Saudi Arabia.

Identifying the type of material inside an object, such as wall systems in building envelopes, can be achieved by seeing through the object using the imaging applications. In addition, seeing through an object is a technique that can be beneficial to many other applications. Military, security, rescue, and building maintenance are among these applications [16]. The idea is that the applied signal has the ability to penetrate walls or objects. For example, high-frequency signals tend to be reflected by solid objects, whereas low-frequency signals pass through objects with a few reflections. In both cases, there is no adequate information that can be extracted from the reflected or passed signals that can indicate the nature of materials inside an object. Seeing through a wall is largely based on recording received signals reflected from moving objects located behind that wall with or without known characteristics [16–22]. Localizing objects behind a wall can be done by various processing methods performed on the received response signals. Ultra-wideband (UWB) signal technology was the main method used [16–22]. Previously, there were some attempts to use Wi-Fi technology [23]. Some studies were conducted to detect what was inside the walls [16–22]. However, the focus of those studies was on transit events, such as moisture concentration [24].

UWB imaging operates in the frequency range of 3.1 GHz to 10.6 GHz [25]. UWB imaging depends on the difference between the dielectric properties of two layers of different materials. The higher this difference is, the more scattered signals are produced. The main properties of UWB signals are their extremely short impulse and maximum output power density, which should be less than -41.3 dBm/MHz. In addition, the bandwidth should be greater than either 500 MHz or 25% of $(1/2)[(f_1 + f_2)/(f_1 + f_2)]$ GHz, where f_1 and f_2 are the lower and upper limits of the frequency bandwidth, respectively. The main advantages of UWB signals in the proposed application are: (a) they have excellent penetration properties, and (b) they have the ability to work well in multipath channels [25]. Usually, the transmitted signal is a Gaussian signal as shown in Fig. 1, while one reflected signal is similar to the signal in Fig. 2.

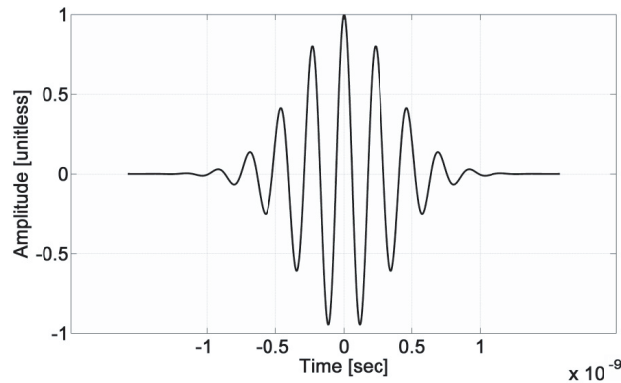


Figure 1. Modulated Gaussian pulse.

As the dielectric properties of the insulation materials that are currently used in building envelopes vary from one to another, the UWB signal can contribute in such applications so as to identify the type of the insulation materials. In this study, a hybrid pattern recognition (HybridPR) method is developed using UWB signal reflection to see inside a wall system in order to determine whether a thermal insulation material exists in such wall systems. The obtained results will help Saudi’s electricity power service provider in determining whether new buildings fulfill the requirements as described in the Saudi building code in order to approve providing electrical services to that building. The next section presents the main method, including sample collection procedure. The obtained results are presented in Section 3.

2. METHODOLOGY

Time Domain is a company that manufactures commercial UWB transceiver. It is used in this research [26]. This device transmits signals with a center frequency of 4.7 GHz and bandwidth of

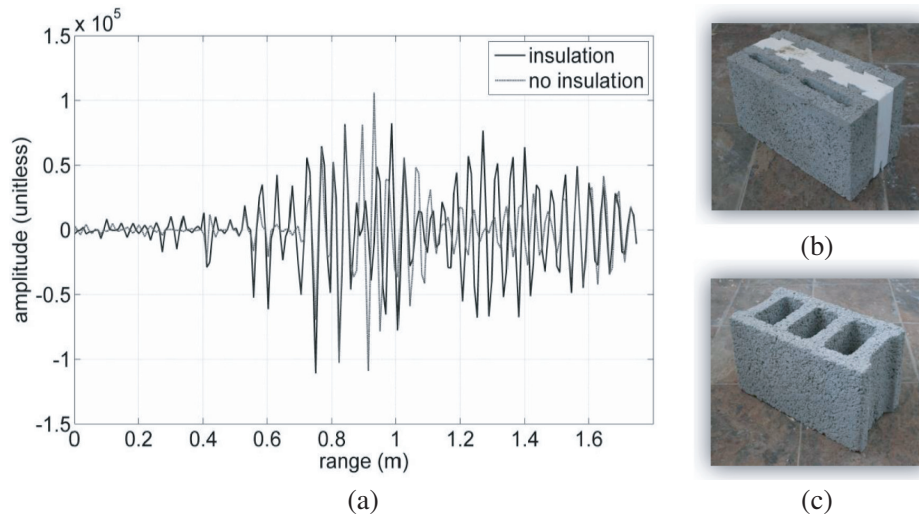


Figure 2. (a) Received scattered signals from insulation and non-insulation walls, (b) insulation material and (c) non-insulation material.

2.5 GHz. It can be configured to work in both mono-static and bio-static configurations.

There are many PR methods that can be used for classification [27]. Artificial neural network or simply neural network (NN), support vector machine (SVM), radial basis function (RBF), decision tree (DT) and classification discriminant (CD), which is a Gaussian based discriminator, are chosen to be investigated. The choices of these techniques are based on their popularity and simplicity of their implementations [27].

The first and probably the most important step in such PR is finding a proper feature vector. For the proposed application, when signal reflections are investigated, there are some features that can be recognized. Fig. 2 shows clear differences between signals when being reflected from walls with and without insulation. It has been decided to use three main groups of features. As shown in Fig. 2, the reflected signals can be divided into three groups. The first group (G1) has raw UWB reflected signals amplitude for the distance from 65 to 110 cm of the signal transceiver. This distance range guarantees that the insulation material will be reached. The second group (G2) contains some main statistics of the UWB reflected signals, which include maximum, minimum, mean, and standard deviation [28], whereas, the third group (G3) contains statistics of the UWB signal envelopes. The statistics of these envelopes include mean, median and std. Table 1 shows these feature vectors. Each group represents complete and separate feature training data samples. Some other signal processing was tried, but the results were not satisfactory. For example, FFT (Fast Fourier Transform) and DCT (Discrete Cosine Transform) were applied to the first group (G1) to reduce the feature vector size. Almost the same result was obtained.

Table 1. Feature vector data for two samples.

	G1: Raw signal	G2: Raw signal statistics $\times 10^4$				G3: Envelope statistics $\times 10^4$		
	Amplitudes	Max	Min	Mean	Std	Mean	Std	Max
Insulation	Fig. 3(a)	8.17	-11.08	-0.19	4.56	5.19	2.98	0.103
No insulation	Fig. 3(b)	7.98	-10.27	-0.017	3.38	2.95	3.21	0.103

2.1. Data Collection

The data were collected from 25 houses in Jubail Industrial City in Saudi Arabia. Each house contains several rooms containing multiple walls that may have different insulation materials. In addition, some

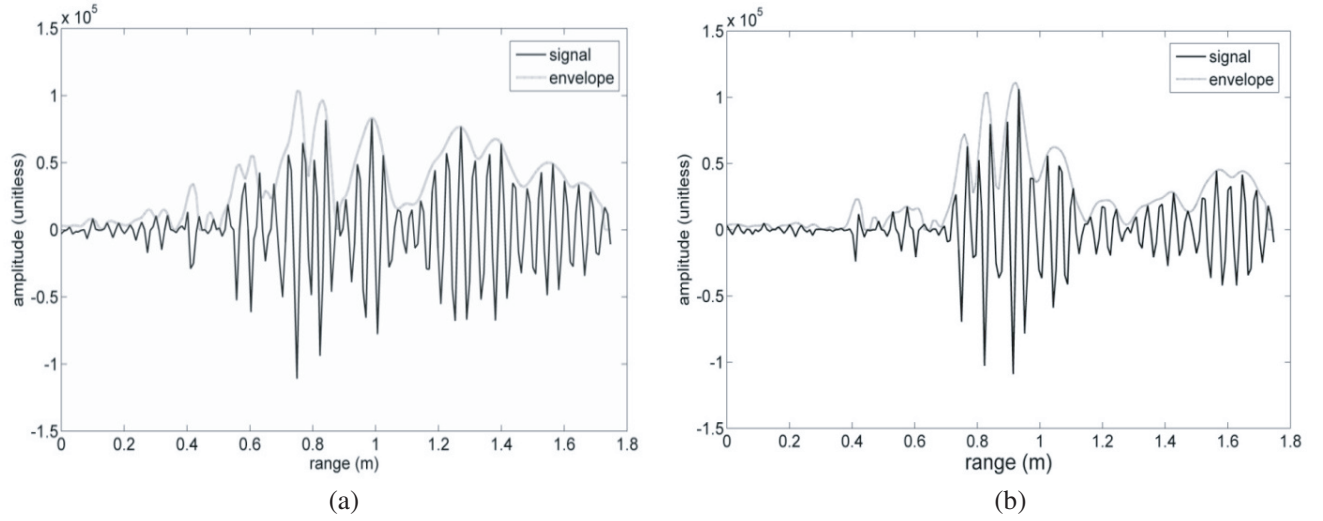


Figure 3. Amplitude and envelope of received signal from walls with (a) insulation materials and (b) no insulation materials.

of these houses do not have thermal insulation. From these houses, 115 different signals were collected. Different types of bricks with and without insulation were used in the building envelopes of these houses. These bricks are red, white, cement with white foam (polystyrene) and, finally, just cement brick without insulation. Dielectric properties of these materials are shown in Table 2 [29–31]. The different types of bricks are shown in Table 3.

Table 2. Dielectric properties for materials used in building walls [29–31].

Type	Dielectric constant (permittivity)
White Brick	3.7–6.0
Red Brick	5.92
White foam (polystyrene)	2.25
Cement Brick	3.7–4.5
Air	1

The UWB Time-Domain transceiver was placed 80 cm away from each wall with a 120 cm height from the ground, as shown in Fig. 4. For each wall, five different signal readings were collected and averaged for better signal to noise cancelation. For each signal transmission, the target, which is the wall material, was recorded.

As the transmitted UWB signals pass through layers with different materials having various dielectric constants, different scattered signals are generated as shown in Fig. 5. These scattered signals are received by the UWB transceiver and recorded as samples of raw signals.

2.2. Hybrid Pattern Recognition

Once the raw signal together with target labels are collected, the feature extraction is performed. Material types and number of collected signals are shown in Table 3. The three different groups of features were constructed. Five different PR models were constructed. The focus was on building appropriate hybrid model rather than individual PR models. For this reason, simple PR models were used. They are NN, SVM, RBF, CD and DT, which were chosen for their simplicity. In all of these

Table 3. Types of insulation materials and the number of collected samples.

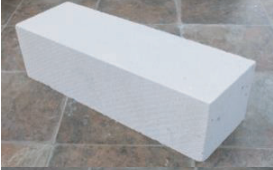
Type	Photo	No. of collected samples
White Brick		32
Red Brick		24
Brick with Foam (polystyrene)		24
Brick without Insulation		35



Figure 4. Experiment setup for collecting the data samples.

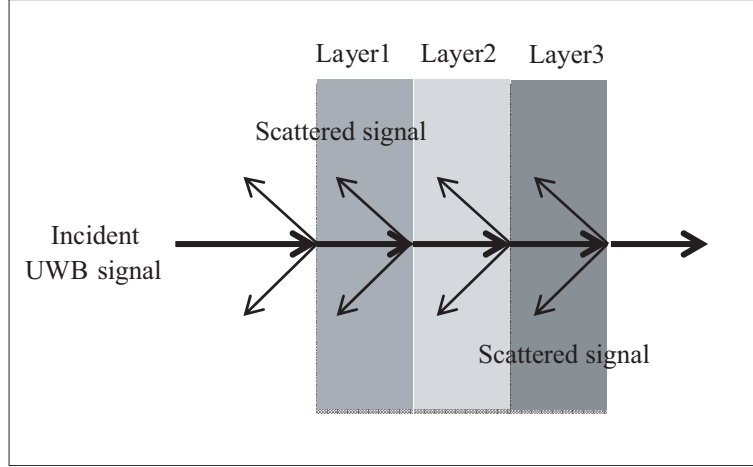


Figure 5. Scattered UWB signals from different wall layers.

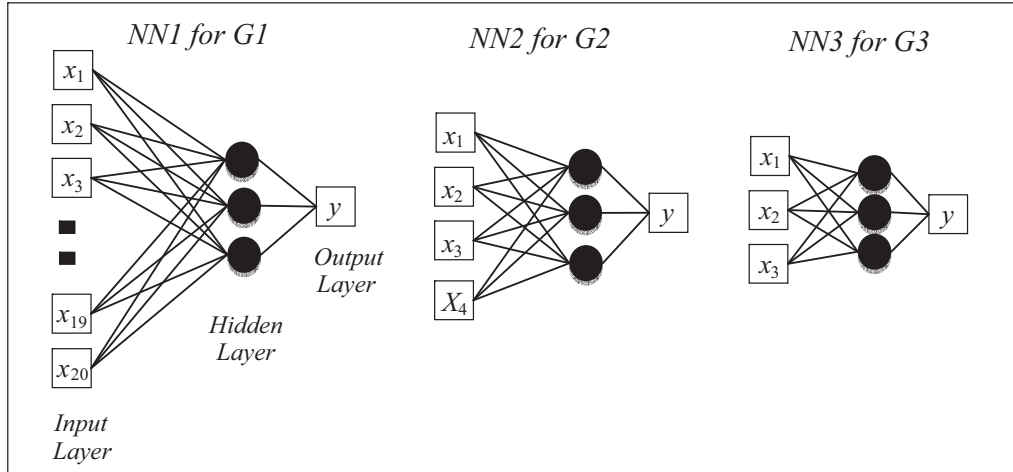


Figure 6. The three NNs topologies.

pattern recognition methods, the learning was supervised learning which is based on the following concept. Consider the mapping:

$$y = w_1x_1 + w_2x_2 + \dots + w_Mx_M = \sum_{j=1}^M w_jx_j$$

$W = [w_1, w_2, \dots, w_M]$ is the weight vector

Let the training data be $\{(X = [x_1^n \dots x_M^n], t^n)\}_{n=1}^N$; n is a label; t^n are the target, defining error $= 1/2 \sum_{n=1}^N \{(y^n - t^n)\}^2$. The goal is to find the best W to minimize E [32].

The NNs were back-propagation feed-forward structures with 20, 4 and 3 input nodes for G1, G2, and G3, respectively, each with one hidden layer containing 3 nodes and tangent transfer function. Fig. 6 shows the topologies of the three neural networks while Table 4 shows the main parameters.

As shown in Tables 3 and 4, the sample data size was 115, and the feature vector sizes were 20, 4 and 3 for NN1, NN2 and NN3, respectively. The data were divided into 3 sets for training, validating and testing. Simple SVM with radial base functions as the kernel functions and sigma values of 1 was used. The RBF parameters are 0.02 as mean square error, 0.91 as spread of radial basis functions,

Table 4. The three NNs main parameters.

NN parameters	NN1	NN2	NN3
No of input nodes	20	4	3
No of Hidden Layers	1	1	1
No of Nodes in Hidden Layer	3	3	3
No of output nodes	1	1	1
Transfer function	tansig	tansig	tansig
Training algorithm	trainlm	trainlm	trainlm
Learning rate	0.3	0.3	0.3
Momentum control	0.65	0.65	0.65
Maximum No. of epochs	250	250	250
Minimum performance gradient	1e-5	1e-5	1e-5
Training set size	75% of total samples	75% of total samples	75% of total samples
Validating set size	15% of total samples	15% of total samples	15% of total samples
Testing set size	15% of total samples	15% of total samples	15% of total samples

Table 5. SVM and RBF main parameters.

SVM parameters	Value	RBF parameters	Value
Kernel function	rbf	Mean square error	0.02
Sigma (standard deviation)	1	RBF spread	0.91
		Maximum No. of neurons	70
Training set size	100%	Training set size	100%
Validating set size	0	Validating set size	0
Testing set size	0	Testing set size	0

and 70 as the maximum number of neurons. Table 5 shows the main parameters for both SVM and RBF. CD is built using a simple Gaussian discriminant analysis model. DT is a linear classification tree built on the training data. Cross validation is used for the neural networks methods. Even through no cross validation was used for SVM, RBF, CD and DT models, the testing set was used to examine the performance and the generalization of these models.

Cross-validating was used only for NNs. For all other methods, testing was performed without cross-validating. To implement training, validating and testing, MATLAB built-in functions were used [33]. Tables 6 and 7 show how the training and testing processes were conducted. The constructed training and target data are referred as '*Train_pattern*' and '*Train_target*', respectively. Fig. 7 shows the training, validating and testing for group 1 NN and construction of group 2 decision tree.

2.3. Detection Procedure

All feature groups are used to build all PR models as in the following steps:

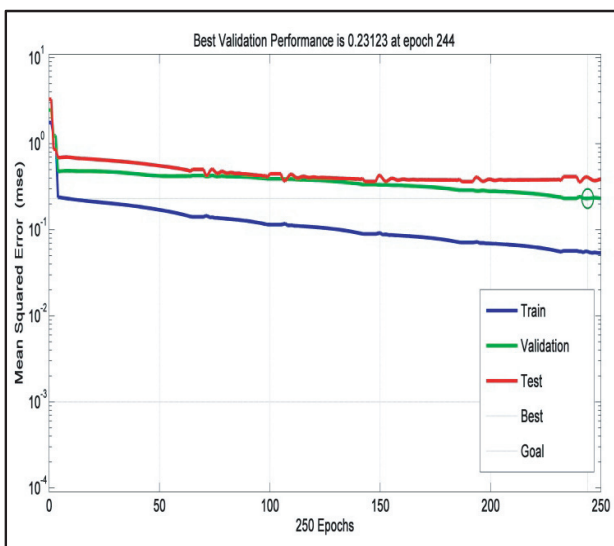
1. G1 samples are used to build NN1, SVM1, RBF1, CD1, and DT1.
2. G2 samples are used to build NN2, SVM2, RBF2, CD2, and DT2.
3. G3 samples are used to build NN3, SVM3, RBF3, CD3, and DT3.
4. The final prediction of PR methods on G1 is based on the majority results of these methods.
5. Similar results are obtained for G2 and G3.
6. The final prediction of the NN model on G1, G2, and G3 is based on majority rule of this NN on these groups.

Table 6. Steps for NN training and testing processes.

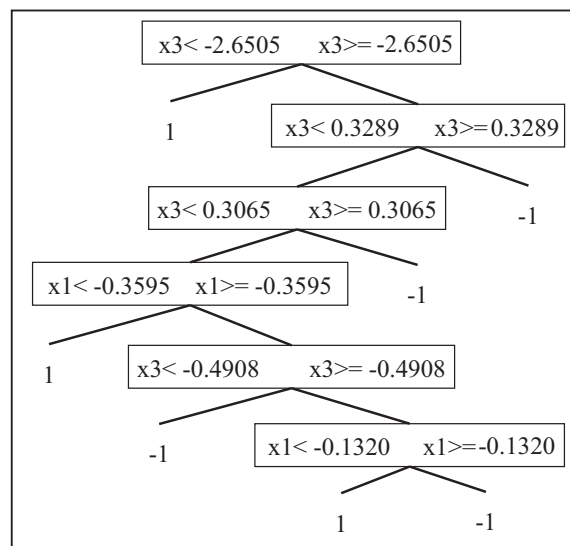
NN	MATLAB code
NN structure (3 nodes in Hidden Layer)	<code>net = feedforwardnet(3,'trainlm');</code>
Learning rate	<code>net.trainParam.lr = 0.3;</code>
Momentum	<code>net.trainParam.mc = 0.65;</code>
Validating fails	<code>net.trainParam.max_fail = 100;</code>
Training set size	<code>net.divideParam.trainRatio = 0.75;</code>
Validating set size	<code>net.divideParam.valRatio = 0.15;</code>
Testing set size	<code>net.divideParam.testRatio = 0.15;</code>
NN initialize	<code>net = init(net);</code>
NN training, validating and testing	<code>[net,tr]=train(net,Train_pattern,Train_target');</code>

Table 7. Steps for SVM, RBF, CD and TD training and testing processes.

Process	MATLAB code
SVM training	<code>svmStruct = svmtrain(Train_pattern,Train_target, 'ShowPlot',false,'kernel_function','rbf','rbf_sigma',1,'BoxConstraint', 1);</code>
SVM testing	<code>res_SVM = svmclassify(svmStruct,Test_pattern,'ShowPlot',false);</code>
RBF training	<code>netRB = newrb(Train_pattern,Train_target',0.02,0.91,70,1);</code>
RBF testing	<code>res_RBF = sim(netRB,Test_pattern');</code>
CD training	<code>linclass = ClassificationDiscriminant.fit(Train_pattern',Train_target');</code>
CD testing	<code>res_CD = predict(linclass,Test_pattern');</code>
DT training	<code>Dtree = classregtree(Train_pattern',Train_target,'method','classification');</code>
DT testing	<code>res_DT = eval(Dtree, Test_pattern');</code>



(a)



(b)

Figure 7. Examples of PR training and testing using MATLAB. (a) NN1, (b) decision tree 2 (DT2) where '1' means insulation exists and '-1' otherwise.

7. Similar results are obtained for SVM, RBF, CD, and DT.
8. A total of 15 predictions are generated. The overall result is based on the majority rule.

There are two main result categories. The first result category is based on data sample groups, while the second result category is based on PR methods. The majority rule (voting rule) is applied to these two categories to obtain the final prediction result. For example, two or more of the outputs of NN1, NN2, and NN3 dominate the result of the first category. In addition, three or more of NN1, SVM1, RBF1, CD1, and DT1 dominate the result of the other category. Other models follow the same pattern for both categories. The training result is shown in Fig. 8. From the 115 samples, 12 samples were arbitrarily chosen as the testing samples. The test samples include all possible types of targets (insulation materials).

The training and testing performance accuracy result was obtained using Eq. (1)

$$Accuracy = \frac{\text{total number of correct detections}}{\text{total number of samples}} \tag{1}$$

It can be noticed that PR methods perform well on G1. NN generally performs well on all groups. DT for G2 and G3, however, shows the lowest performance. In spite of these notes, the overall performance result is satisfactory.

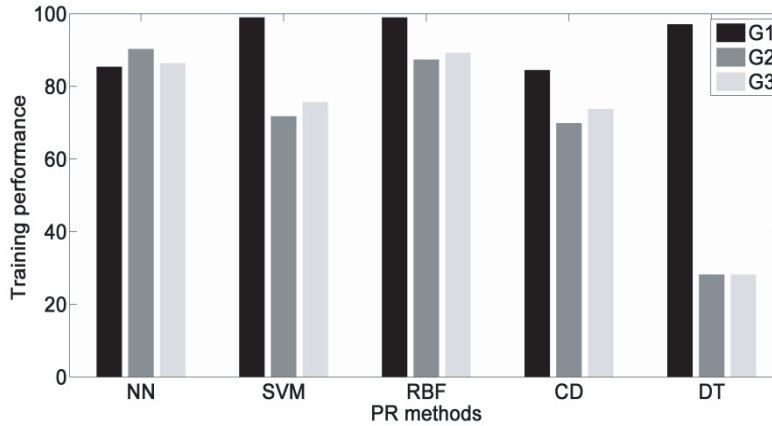


Figure 8. Training performance result.

2.4. Enhanced Method

One enhancement can be done by performing a result analysis on these PRs and sample groups. It was found that some of these PRs and sample groups resulted in high performance accuracy. Based on the training results shown in Fig. 8, weighted output with confidence percentage is calculated and presented together with the majority rule output result. The weighted result is calculated using Eq. (2).

$$ConfPerformance = \frac{\sum_{i \in G_S, j \in PatModels} B * TP_{ij}}{\sum_{i \in G_S, j \in PatModels} TP_{ij}} \tag{2}$$

where G_s : are the training groups samples, B : 1 if model i produces 1 for group j , 0 otherwise, TP : the training performance result, $PatModels$: are NN, SVM, RBF, CD and DT.

3. RESULTS

The work was conducted using MATLAB. The GUI was built for better presentation. Screen shots are shown in Figs. 9(a) and (b) for two of the test samples. Additionally, the offline prediction performance of the system for each model on each data group varies, as shown in Table 8. As shown in Table 8 and

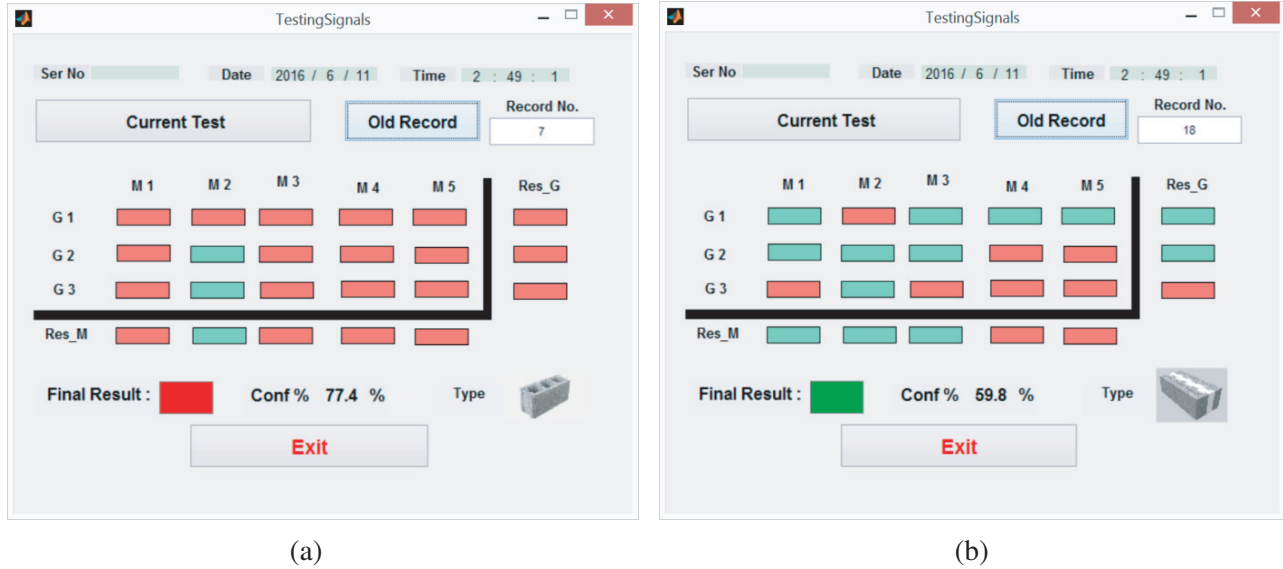


Figure 9. GUI showing prediction result of (a) wall with no insulation material and (b) wall with insulation material.

Table 8. Testing performance result.

	G1	G2	G3	All groups
NN	100	91.7	100	100
SVM	100	58.3	75.0	75.0
RBF	100	83.3	83.3	83.3
CD	100	58.3	75.0	83.3
DT	100	41.7	41.7	41.7
HybridPR	100	83.3	91.7	100

Fig. 8, good results were obtained using G1. For G2 and G3, there are some low performance results (e.g., see the case for DT). However, when the HybridPR method was used, the results reached 95% on training samples and full correct prediction of existence and type of insulation on the testing samples. This was based on testing the system using 10% of the collected samples, which was set aside for this purpose. The performance of each PR on G1 is up to 100%. However, it cannot be fully generalized, as the size of the training samples is not large enough.

4. CONCLUSION

Prediction of the type of wall materials was investigated using PR methods. A HybridPR was constructed using these methods and showed better performance than each individual presented method. The training samples were collected from 25 houses. The features were obtained based on UWB scattered signal envelope characteristics, raw signals, and signal statistics. The HybridPR reached nearly 100% correct predictions of the existence and types of insulation materials, respectively. The training and testing sample sizes can be enlarged for better confidence in the results.

REFERENCES

1. U.S. Energy Information Administration 2011–2012, Available on line: <http://www.eia.gov/todayinenergy/detail.cfm?id=10271/> (accessed on 26 August 2016).

2. Vrachopoulos, M. G., M. K. Koukou, D. G. Stavlas, V. N. Stamatopoulos, A. F. Gonidis, and E. D. Kravaritis, "Testing reflective insulation for improvement of buildings energy efficiency," *Central European Journal of Engineering*, Vol. 2, 83–90, 2012.
3. Green Public Procurement Thermal Insulation Technical Background Report, Report for the European Commission — DG Environment by AEA, Harwell, June 2010, Owner, Editor: European Commission, DG Environment-G2, B-1049, Brussels.
4. Saber, H. H., W. Maref, M. C. Swinton, and C. St-Onge, "Thermal analysis of above-grade wall assembly with low emissivity materials and furred-airspace," *Journal of Building and Environment*, Vol. 46, 1403–1414, 2011.
5. Saber, H. H., M. C. Swinton, P. Kalinger, and R. M. Paroli, "Long-term hygrothermal performance of white and black roofs in North American climates," *Journal of Building and Environment*, Vol. 50, 141–154, 2012.
6. Saber, H. H., M. C. Swinton, P. Kalinger, and R. M. Paroli, "Hygrothermal simulations of cool reflective and conventional roofs," *Proceedings of the 2011 International Roofing Symposium*, Washington, D.C., September 06–11, 2011.
7. Saber, H. H., W. Maref, G. Sherrer, and M. C. Swinton, "Numerical modeling and experimental investigations of thermal performance of reflective insulations," *Journal of Building Physics*, Vol. 36, 163–177, 2012.
8. Saber, H. H., W. Maref, A. H. Elmahdy, M. C. Swinton, and R. Glazer, "3D heat and air transport model for predicting the thermal resistance of insulated wall assemblies," *Journal of Building Performance Simulation*, Vol. 5, 75–91, 2012.
9. Maref, W., H. H. Saber, R. Glazer, M. M. Armstrong, M. Nicholls, A. H. Elmahdy, and M. C. Swinton, "Energy performance of highly insulated wood-frame wall systems using a VIP," *10th International Vacuum Insulation Symposium*, Ottawa, Ontario, September 15–11, 2011.
10. Saber, H. H., W. Maref, A. H. Elmahdy, M. C. Swinton, and R. Glazer, "3D thermal model for predicting the thermal resistance of spray polyurethane foam wall assemblies," *11th International Conference on Thermal Performance of the Exterior Envelopes of Whole Buildings XI*, Clearwater, FL, USA, December 05–10, 2010.
11. Elmahdy, A. H., W. Maref, H. H. Saber, M. C. Swinton, and R. Glazer, "Assessment of the energy rating of insulated wall assemblies — A step towards building energy labeling," *10th International Conference for Enhanced Building Operation*, Kuwait, October 26–10, 2010.
12. Elmahdy, A. H., W. Maref, M. C. Swinton, H. H. Saber, and R. Glazer, "Development of energy ratings for insulated wall assemblies," *2009 Building Envelope Symposium*, San Diego, CA, October 26–09, 2009.
13. Saber, H. H., W. Maref, A. H. Elmahdy, M. C. Swinton, and R. Glazer, "Energy rating of insulated wall assemblies," *Construction Innovation*, Vol. 15, 1, 2010.
14. ASTM 2006, ASTM C-1363, Standard test method for the thermal performance of building assemblies by means of a hot box apparatus, 2006 Annual Book of ASTM Standards 04.06:717–59, <http://www.astm.org> (accessed on 26 August 2016).
15. Madding, R., "Finding R-values of stud frame constructed houses with IR thermography," *InfraMation 2008 Proceedings ITC*, 126 A, 2008.
16. Riaz, M. M. and A. Ghafoor, "principle component analysis and fuzzy logic based through wall image enhancement," *Progress In Electromagnetics Research*, Vol. 127, 461–478, 2012.
17. Zhu, F., et al., "Low-profile directional ultra-wideband antenna for see-through-wall imaging applications," *Progress In Electromagnetics Research*, Vol. 121, 121–139, 2011.
18. Kocur, D., M. Svecova, and J. Rovnakova, "through-the-wall localization of a moving target by two independent UltraWideband (UWB) radar systems," *Sensors*, Vol. 13, 11969–11997, 2013.
19. Jia, Y., L. J. Kong, and X. B. Yang, "A novel approach to target localization through unknown walls for through-the-wall radar imaging," *Progress In Electromagnetics Research*, Vol. 119, 107–132, 2011.

20. Zhai, S. and T. Jiang, "Target detection and classification by measuring and processing bistatic UWB radar signal," *Measurement*, Vol. 47, 547–557, 2014.
21. Lu, T., K. Agarwal, Y. Zhong, and X. Chen, "Through-wall imaging: Application of subspace-based optimization method," *Progress In Electromagnetics Research*, Vol. 102, 351–366, 2010.
22. Kumar, P. and T. Kumar, "UWB impulse radar for through-the-wall imaging," *International Journal of Electromagnetics and Applications*, Vol. 1, 19–23, 2011.
23. Adib, F. and D. Katabi, "See through walls with Wi-Fi!," *ACM SIGCOMM'13*, Hong Kong, August 2013.
24. Healy, W. M., "Detection of moisture accumulation in wall assemblies using ultra-wideband radio signals," *Proceedings of Performance of Exterior Envelopes of Whole Building IX International Conference*, December 5–10, Clearwater Beach, FL, 2004.
25. Oppermann, I., M. Hamalainen, and J. Linatti, *UWB: Theory and Applications*, 1st Edition, Wiley, 2004.
26. Time domain corporation, Comings Research Part, 330 Wynn Drive, Suite 300, Hantsville, Al 358.
27. Khodjet-Kesba, M., K. Chahine, K. Drissi, and K. Kerroum, "Comparison of ultra-wideband radar target classification methods based on complex natural resonances," *PIERS Proceedings*, Kuala Lumpur, Malaysia, March 27–30, 2012.
28. Reza, K. J., S. Khatun, F. Mohd, and M. N. Morshed, "Performance enhancement of UWB breast cancer imaging system: Proficient feature extraction and biomedical antenna approach," *2nd International Conference on Electronic Design*, Penang, Malaysia, August 19–21, 2014.
29. Microwave Encyclopedia 2001–2016, Available on line : <http://www.microwaves101.com/encyclopedias/miscellaneous-dielectric-constants/> (accessed on 26 August 2016).
30. Wilson, R., "Propagation losses through common building materials: 2.4 GHz vs 5 GHz, reflection and transmission losses through common building materials," *Technical Repo E10589*, Magic Networks Inc., 2002.
31. Makul, N., P. Rattanadecho, and D. Agrawal, "Application of microwave energy in cement and concrete — A review," *Renewable and Sustainable Energy Reviews*, 2014.
32. Theodoridis, S. and K. Koutroumbas, *Pattern Recognition*, 4th Edition, Academic Press, 2008.
33. MATLAB and Neural Network Toolbox Release 2012b, TheMathWorks, Inc., Natick, Massachusetts, United States.